Journal of Biomechanics 47 (2014) 3868–3875

Contents lists available at ScienceDirect

Journal of Biomechanics

journal homepage: www.elsevier.com/locate/jbiomech
www.JBiomech.com

Mechanical instability of normal and aneurysmal arteries

Avione Y. Lee [1], Arnav Sanyal [1], Yangming Xiao, Ramsey Shadfan, Hai-Chao Han *

Department of Mechanical Engineering, The University of Texas at San Antonio, Biomedical Engineering Program, UTSA-UTHSCSA, San Antonio, TX, United States

ARTICLE INFO

Article history:
Accepted 6 October 2014

Keywords:
Aneurysm
Stability
Tortuosity
Critical buckling pressure
Post-buckling
Wall stress
Deformation
Aorta
Artery

ABSTRACT

Tortuous arteries associated with aneurysms have been observed in aged patients with atherosclerosis and hypertension. However, the underlying mechanism is poorly understood. The objective of this study was to determine the effect of aneurysms on arterial buckling instability and the effect of buckling on aneurysm wall stress. We investigated the mechanical buckling and post-buckling behavior of normal and aneurysmal carotid arteries and aorta's using computational simulations and experimental measurements to elucidate the interrelationship between artery buckling and aneurysms. Buckling tests were done in porcine carotid arteries with small aneurysms created using elastase treatment. Parametric studies were done for model aneurysms with orthotropic nonlinear elastic walls using finite element simulations. Our results demonstrated that arteries buckled at a critical buckling pressure and the post-buckling deflection increased nonlinearly with increasing pressure. The presence of an aneurysm can reduce the critical buckling pressure of arteries, although the effect depends on the aneurysm's dimensions. Buckled aneurysms demonstrated a higher peak wall stress compared to unbuckled aneurysms under the same lumen pressure. We conclude that aneurysmal arteries are vulnerable to mechanical buckling and mechanical buckling could lead to high stresses in the aneurysm wall. Buckling could be a possible mechanism for the development of tortuous aneurysmal arteries such as in the Loeys–Dietz syndrome.

1. Introduction

Rupture of abdominal aortic aneurysms (AAA) is the thirteenth leading cause of death in the United States (Vorp, 2007). Extensive biomechanical studies have shown that highly elevated local stress and weakened aneurysm wall make aneurysms vulnerable to rupture (Fillinger et al., 2002,2003; Vorp, 2007; Rodriguez et al., 2008).

Aneurysms are often associated with vessel tortuosity (Hatakeyama et al., 2001; Wolf et al., 2001; Fillinger et al., 2004; Vorp, 2007). For example, in patients with Loeys–Dietz syndrome, the carotid and cerebral aneurysms tend to be tortuous (Loeys et al., 2006; Johnson et al., 2007). Around 10% of Loeys–Dietz syndrome patients also have abdominal aortic aneurysms, which may become tortuous as well (Wolf et al., 2001; Johnson et al., 2007). It has been suggested that artery tortuosity may lead to aneurysm formation (Deterling, 1952; Arends et al., 2008) and aneurysmal tortuosity has been proposed as a risk factor for aneurysm rupture (Del Corso et al., 1998; Sacks et al., 1999; Fillinger et al., 2003; Pappu et al., 2008; Rodriguez et al., 2008; Georgakarakos et al., 2010). Therefore, it is important to better understand the relation between artery tortuosity and aneurysms.

Recent studies from our lab suggested that artery buckling, the loss of mechanical stability due to hypertension, decreased axial stretch ratio and elastin degradation in the wall, can lead to vessel tortuosity (Han, 2007, 2009a; Lee et al., 2012; Han et al., 2013). However, the mechanical stability of aneurysmal arteries and the post-buckling behavior of normal and aneurysmal arteries have not been investigated. Therefore, the objective of this study was to investigate the buckling and post-buckling behavior of normal and aneurysmal arteries and the effects of buckling on the wall stress in aneurysmal arteries.

2. Methods

The effects of aneurysms on arterial stability were evaluated by simulating the buckling and post-buckling behavior of normal and aneurysmal arteries using finite element analysis. Simulation results were compared with theoretical estimations and experimental measurements of porcine carotid arteries for validation.

2.1. Buckling analysis of normal arteries

Six cylindrical arterial wall models were created using Solidworks® (Dassault Systèmes, Waltham, MA) based on the specific dimensions of six normal porcine

* Corresponding author at: Department of Mechanical Engineering, The University of Texas at San Antonio, San Antonio, TX 78249, United States.
Tel.: +1 210 458 4952; fax: +1 210 458 6504.
E-mail address: hchan@utsa.edu (H.-C. Han).
[1] These authors contributed equally to this work.

http://dx.doi.org/10.1016/j.jbiomech.2014.10.010
0021-9290/

carotid arteries with diameters in the range of 4.5–7 mm and length in the range of 50–63 mm obtained in our previous study (Lee et al., 2012). The arterial wall was modeled as a homogenous, incompressible, orthotropic, nonlinear material with the Fung strain energy function of the form (Fung, 1993):

$$w = \frac{b_0}{2}e^{Q} \tag{1a}$$

$$Q = b_1E_\theta^2 + b_2E_z^2 + b_3E_r^2 + 2b_4E_\theta E_z + 2b_5E_zE_r + 2b_6E_\theta E_r \tag{1b}$$

where b_1, b_2, b_3, b_4, b_5, b_6, and b_0 are material constants. Subscripts r, θ, z represents the radial, circumferential and axial directions, respectively, which have different mechanical stiffness (orthotropic). Although the material constants for these porcine carotid arteries were obtained in our previous study (Lee et al., 2012), they did not satisfy the convexity requirement of the strain energy density function for finite element analysis (Sacks and Sun, 2005; Datir et al., 2011). Thus, we re-determined the material constants with the following restrictions to ensure convexity (Lee, 2011; Lee et al., 2012):

$$b_i > 0, \quad i = 1, 2, \ldots, 6 \tag{2a}$$

$$b_1 + b_2 > 2b_4; \quad b_2 + b_3 > 2b_5; \quad b_3 + b_1 > 2b_6; \tag{2b}$$

The new set of convex material constants are listed in Table 1. Out of the six arteries, one artery (artery E6 in Table 1) was also treated with elastase over its entire length to obtain material constants of a weak arterial wall as described in our previous study (Lee et al., 2012).

The buckling behavior of all arterial models was simulated using the commercial FEA package ABAQUS® (v6.10, Dassault Systèmes, Waltham, MA). The arterial models were meshed using hybrid, linear hexahedral elements. Since arteries are under significant longitudinal strain in vivo (Han and Fung, 1995; Han et al., 2003), a designated axial displacement was first applied to all nodes at the distal end of the arteries to achieve the given stretch ratios. Then, a static internal pressure was applied to the lumen of the arterial models and the external pressure was set at zero. Both ends of the arteries were assumed as fixed with no lateral displacement or rotation, but were allowed to expand radially. A small initial bend of 1 degree along the central axis of the arteries was created as an imperfection to facilitate the buckling analysis. A series of different bend angle were used in a pilot study and the results showed that the variations in the small initial angle had no effect on the critical buckling pressure results (Datir et al., 2011; Lee, 2011).

The maximum lateral deflection of the central axis of a model artery was determined by averaging the deflections of the two edges of the wall at the mid-point of the vessel and was plotted against the lumen pressure. The pressure at which the deflection starts to increase from baseline (zero) and reaches a small value of 0.5 mm was defined as the critical buckling pressure. This definition was consistent with the criteria used in our previous experimental studies on artery buckling (Lee et al., 2012; Liu and Han, 2012). The critical buckling pressure was also determined from theoretical buckling equation for comparison (Han, 2009a; Lee et al., 2012).

2.2. Buckling analysis of aneurysmal arteries

Aneurysmal arterial models were created by adding a spherically shaped dilation (fusiform aneurysm) at the middle segment of a normal cylindrical artery model (control). The control model was created with an outer diameter of 6 mm, wall thickness of 1 mm, and total length of 100 mm. Idealized symmetric aneurysms were drawn with various aneurysm diameter (D_A), aneurysm length (L_A), and aneurysm wall thickness t_A while the total length of the vessels were kept at 100 mm (the neck lengths were determined by 2 L_N=total length L—aneurysm length L_A accordingly) (Fig. 1) to investigate the effect of aneurysm dimensions (shape and size) on the critical buckling pressure and wall stress. The length and diameter of the aneurysm was varied in the range of 6–36 mm to determine the effect of different aneurysm sizes and shapes. Aneurysm wall thickness was assumed as either the same as the normal artery (1 mm, uniform wall) or half the wall thickness of a normal artery (0.5 mm, thin wall). In addition, an asymmetric aneurysm model was created with dilation on one side of the vessel with an aneurysm length of 18 mm, aneurysm diameter of 12 mm and wall thickness of 1 mm.

Table 1
Convex material constants of six normal porcine carotid arteries and one elastase-treated artery (refit of experimental data from Lee et al., 2012).

Artery ID	b_0	b_1	b_2	b_3	b_4	b_5	b_6
5	20.42	0.679	0.751	0.228	0.0519	0.033	0.051
6	18.14	0.470	0.460	0.150	0.090	0.060	0.030
7	33.04	0.461	0.588	0.266	0.123	0.083	0.087
8	13.35	0.827	0.547	0.613	0.018	0.072	0.027
9	16	0.820	0.771	0.509	0.116	0.092	0.046
E6	30.69	1.265	0.353	1.000	0.179	0.011	0.026
E6 treated	3.07	3.375	0.940	0.564	0.179	0.007	0.090

Note: "E6 treated" is the same artery as E6, but after elastase treatment to remove elastin in the wall (see Lee et al. (2012) for details).

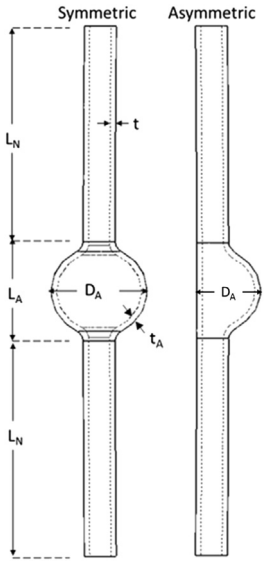

Fig. 1. Geometric models of symmetric (left) and asymmetric (right) shaped aneurysmal arteries. The aneurysm length, diameter, and thickness are denoted as L_A, D_A, and t_A. The neck length of the vessel is $2L_N$.

The arterial and aneurysm wall were assumed to behave as a homogenous, incompressible, and orthotropic nonlinear material as described by Fung strain energy function with material constants given in Table 1. The aneurysm wall was assumed to have either the same material constants as the normal arterial wall (artery E6 in Table 1) or was assumed to have the material constants of the elastase-treated (weakened) arterial wall (artery "E6 treated" in Table 1) (Lee et al., 2012). This allowed us to compare normal and weakened aneurysmal walls.

To determine the effect of buckling on aneurysmal wall stress, we compared two models with identical aneurysms (L_A=D_A=18 mm) but different neck lengths (a long neck with L_N=41 mm and a short neck with L_N=6 mm). By changing neck lengths, the two models had different critical buckling pressures, thus at physiological pressure, the aneurysm with the long neck buckled while the control one with the short neck remained un-buckled. The buckling behavior and aneurysm wall stress in the long and short models were determined for the set of six material constants for the normal arteries listed in Table 1.

2.3. Buckling analysis of tapered abdominal aorta with an aneurysm

To further illustrate the buckling behavior of abdominal aortic aneurysms, a model of a tapered abdominal aorta was created with a lumen diameter of 17 mm at the proximal end, 14 mm at the distal end, wall thickness of 1.5 mm and length of 123 mm. These dimensions were based on previously reported average measurements of human abdominal aortas (Fleischmann et al., 2001) and is a linear approximation of the actual changes in diameter and wall thickness along the aorta (Liu and Fung, 1988; Han and Fung, 1991). A fusiform aneurysm of 30 mm in diameter and 40 mm in length was created in the middle of the aorta. The wall thickness of the aneurysm was assumed to be either the same as the normal aorta (1.5 mm, uniform wall) or half the wall thickness of the normal aorta (0.75 mm, thin wall). Since human data is not available, the aorta wall was assumed to be of an orthotropic nonlinear material with Fung strain energy function with material constants of a porcine carotid artery (artery "E6" in Table 1). The aneurysm wall was assumed to have either the same material constants as the normal aorta wall or the material constants of the elastase-treated arterial wall (artery "E6 treated" in Table 1, weak wall) as specified.

2.4. Experimental measurement of post-buckling behavior of arteries

We measured the deflection from pre- to post-buckling of the set of six normal porcine carotid arteries listed in Table 1 using the method previously described (Martinez et al., 2010; Lee et al., 2012). Briefly, the displacements of the two edges of the arterial wall were determined from recorded buckling videos and photos using Image Pro Plus®. Then the maximum deflections of the central axis of the arteries were determined by averaging the displacements of the two edges of the wall measured at the middle points of the vessels. The experimental deflections were compared with the computational results.